ISSN 1392-1207. MECHANIKA. Vol. 30, No. 5, 2024: 458–465

A New Two-Phase Design Process for a Compliant Mechanism Gripper

Gopal VIJAYAN*, Bharanidaran RAMALINGAM, Libu George BABU***, Alphin MASILAMANY SANTHA******

**KCG College of Technology, Chennai, India, E-mail: gopal@kcgcollege.com*
***Vellore Institute of Technology, Vellore, India, E-mail: bharanidaran.r@vit.ac.in*
****Vellore Institute of Technology, Vellore, India, E-mail: libugeorge.b2016@vitstudent.ac.in*
*****SSN College of Engineering, Chennai, India, E-mail: alphinms@ssn.edu.in*

https://doi.org/10.5755/j02.mech.33592

1. Introduction

In recent years, there has been a widespread application of micro/meso devices in fields such as robotics [1], micro/nano manipulation [2], and precision engineering [3]. These devices are characterized by their small size, susceptibility to damage, intricate assembly processes, and unpredictable performance. To address these challenges, compliant mechanisms have emerged as a suitable mechanism concept.

A compliant mechanism is defined as a mechanism that leverages the elastic properties of materials to transmit forces or displacement from one point to another. When designing micrograppers, a monolithic structure produced through compliant mechanisms is highly favoured. Various techniques have been employed in the design of compliant mechanisms, including mechanism synthesis [4,5], the Pseudo Rigid Body Model (PRBM) [4], optimization techniques [6,7], inverse methods [8], and intuitive gripper design [9]. These approaches contribute to overcoming the complexities associated with micro/meso devices, enhancing their reliability and performance. Recent research efforts have focused on integrating compliant mechanisms into the design of forceps, specifically for robot-assisted applications that demand precise manipulation [10]. M.B. Hong has presented a forceps design with two degrees of freedom, employing a kinematic approach that involves synthesizing a model with dual torsional springs [11].

Enhancing the performance and efficacy of both traditional and robotic surgical methods now requires the refinement of surgical equipment [12–13]. Numerous studies have demonstrated that compliant mechanisms contribute to more successful surgical procedures, as they necessitate less setup and are easier to sterilize [14]. Various investigations have focused on the development of forceps or grippers with unique designs, actuation techniques, or control methods. Traditional rigid link mechanisms, utilizing multiple rigid components and joints to transmit motion from input to output, are commonly employed for forceps creation. While conventional forces are consistent and robust, they exhibit limited accuracy and precision in movements. Additionally, adapting them to micro sizes for application in minimally invasive surgery (MIS) leads to increased complexity and laborious efforts [15].

The utilization of topology optimization has been widespread in research for the design of forceps. Kota et al. [14] propose the application of topology optimization to craft a compliant gripper tailored for positioning and manipulating kidneys during robot-assisted surgery. The development of three-dimensional topology optimization was essential for designing multifunctional forceps capable of both grabbing and cutting activities [16]. Libu introduced a topologically optimized multipurpose gripper con-structed in three separate pieces, later assembled to form the final product [17]. De Lange, D.J., et al. [18] employed topology optimization to create a laparoscopic grasper featuring a highly compliant negative-stiffness compensating mechanism with force feed-back. Additionally, an origami-based compliant grip-per with four degrees of freedom (DOF) was developed, generating translational and rotational motions, including twisting capabilities [19]. Notably, only a limited number of studies have integrated force sensing capabilities into compliant surgical forceps, particularly within robotic surgical systems. The precise measurement of force during surgical procedures is crucial for ensuring controlled manipulation and avoiding damage to soft tissues. Tholey et al. [20] introduced a laparoscopic compliant grasper that can measure force in three directions, comparing both direct and indirect measurement methods. While integrating sensors into surgical instruments adds complexity and challenges to sterilization, accurate force measurement is essential despite potential error accumulation. In addressing these challenges, Zhao and Nelson [20] proposed a novel approach using motor current for force sensing in a tool-tissue interaction concept. This method demonstrated satisfactory results in terms of time delay and accuracy, paving the way for haptic feedback-based robotic surgical systems that remain compatible with existing sterilization methods. Some cable-actuated forceps utilize indirect force sensing, estimating force based on cable pretension and employing dynamic techniques with an unscented Kalman filter [21]. Although these methods provide feedback on tissue properties, their accuracy is limited by factors such as grasper model precision, deviation measurement, signal transmission disturbances, and other elements. An alternative approach involves the use of a traditional fin ray design with modified rigid nodes to estimate intrinsic force sensing without tactile sensors. Experimental techniques employing this design demonstrated an error rate within 8% [22]. This innovative method offers a potential solution to the challenges associated with accurate force measurement in surgical procedures.

This study aims to employ a two-phase design approach for the development of compliant mechanical forceps. The distributed compliant mechanism is achieved through the application of a topology optimization technique, effectively eliminating stress concentration points in the initial conceptual design. The thickness of the forceps is

subsequently deter-mined by parameterizing these conceptual designs. To create a comprehensive prototype, the final design is fabricated, incorporating the handle. The direct measuring approach is considered the most accurate method for determining mechanical properties. To assess the gripping power during operation, a dedicated sensor system has been devised for quantifying the forceps' performance.

2. Design of Microgripper

Designing a microgripper poses a significant challenge due to the intricate nature of handling objects at the micron level with precision. Traditional rigid-body mechanisms become impractical at this scale, as they are challenging to manufacture, handle, and assemble. Consequently, the adoption of compliant-based mechanism design emerges as a more suitable approach for micron-scale grippers. Compliant mechanisms can be categorized into partially compliant and fully compliant mechanisms, depending on the nature of the members involved. Partially compliant mechanisms incorporate rigid mechanical members and conventional joints in conjunction with flexible elements. On the other hand, fully compliant mechanisms exclusively consist of flexible members that achieve mobility through elastic deformation. Compliant members enable elastic deformation by concentrating strains in specific regions or by distributing strains more uniformly throughout the structure. This design choice enhances the feasibility and effectiveness of microgrippers, providing the necessary flexibility and precision required for handling objects at the micron scale.

2.1. Topology optimization

Topology optimization is a logical approach that improves material distribution within a predefined initial design area, considering specified loading and boundary conditions. The aim is to achieve a desired objective function without the need for predefined configuration, as is the case with the kinematic approach involving rigid link mechanisms. The initial design domain, illustrated in Fig. 1, is structured according to the dimensions of forceps used in Minimally Invasive Surgery (MIS) and open surgery.

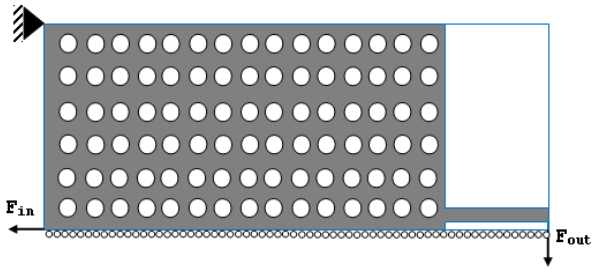

Fig. 1 Initial design domain with pattern of holes

The left top corner of the design domain is constrained with all degrees of freedom, the input force F_{in} is applied at the bottom of the left side edge and symmetric boundary conditions are applied at bottom edge of the design. The output force (F_{out}) is assumed to be acting on the tip of the jaws of the gripper. The finite element model of the initial design domain is developed by discretizing the domain into 150 numbers of elements horizontally and 50 numbers of elements vertically.

The optimized design obtained through this method, when applied to the same loading and boundary, results in a lumped mass design. This configuration is susceptible to stress concentration, posing a risk of design failure. To address this issue, a distributed compliant mechanism is desired. To achieve such a mechanism, a pattern of holes is incorporated. In the initial design domain, it is assumed that no materials are present in these holes. Fig. 1 depicts an exaggerated model. There are approximately thirteen holes in the model, which restricts the local distribution of materials. This configuration enables material distribution through the gaps, resulting in the creation of distributed compliant mechanisms.

The formulation of the topology optimization problem involves expressing the objective function [4], as shown in equation (1). In the perspective of a static topology optimization problem, the goal is to ascertain the optimal material distribution within a structure. This optimization aims to enhance a specific objective function while considering given loads and support conditions, all while adhering to a predetermined volume constraint (reducing volume by 70%). In the present research, the primary objective function is to maximize the ration of Mutual Strain Energy (MSE) to total strain energy of input and output loads.

$$Maximize\left(\frac{MSE}{SE_1+SE_2}\right)=$$

$$=\frac{U_1^{\,T}KU_2}{U_1^{\,T}KU_1+U_2^{\,T}KU_2}=$$

$$=\sum_{e=1}^{N}\left(x_e\right)^p\frac{u_{e1}^{\,T}k_o u_{e2}}{\left(u_{e1}^{\,T}k_o u_{e1}+u_{e2}^{\,T}k_o u_{e2}\right)}. \qquad (1)$$

Subject to:

$$:\frac{V(x)}{V_o}=f,$$

$$:[K]\{U\}=\{F\},$$

$$:X_{min}\le x\le 1,$$

where $\{U\}$ represents global displacement vectors, $\{F\}$ represents global force vectors, $[K]$ represents global stiffness matrix $\{u_{el}\}$ represents an element displacement vector due to F_{in} at input port, $[k_e]$ represents stiffness matrix of the element $\{u_{e2}\}$ represents an element displacement vector due to F_{out} at output port, x represents vector of design variables, x_{min} is the minimum relative densities (in the MATLAB program, non-zero value has been assumed to avoid singularity), N is the number of elements, p is the penalization power (typically p = 3), $V(x)$ represents the material volume, V_o is the design domain volume, f is the volume fraction (volfrac).

The topology optimization code executed using MATLAB software [3], with necessary modifications applied to the existing code. The outcome, after 264 iterations, is depicted in Fig. 2, showcasing a topologically optimized design. In contrast, Fig. 3 illustrates the optimized result without a pattern of holes. The comparison between the two figures distinctly reveals that in the absence of holes, the de-

sign exhibits as a lumped type of mechanism. The introduction of a pattern of holes in the initial design imposes constraints on the grouping of a larger number of elements. Consequently, this leads to the emergence of a distributed compliant design. This distributed mechanism not only enhances manufacturability but also mitigates stress concentration spots, contributing to the creation of a simplified design.

It is noteworthy that the process of converting the MATLAB output to a CAD model requires human intervention. Fig. 2 exposes certain regions where the material is not distributed densely; rather, it appears as disconnectivity or thin connectivity. These shortcomings, however, can be rectified through human intervention, guided by engineering insight. The intervention process aids in addressing issues such as disconnectivity and thin connectivity, thereby refining the overall design output. This nuanced approach ensures that the final design aligns more closely with engineering principles and requirements.

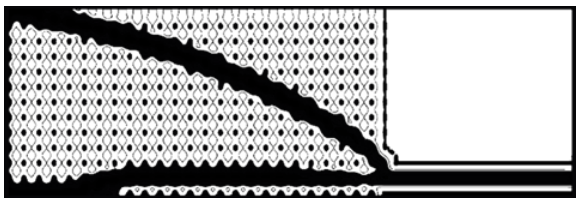

Fig. 2 Topologically optimized results with pattern of holes

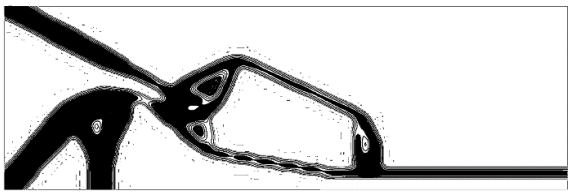

Fig. 3 Topologically optimized domain without pattern of holes

2.2. Design of thickness

In the development of planar mechanisms, topology optimization is often employed to optimize material distribution within a given space. However, determining the appropriate thickness of components for specific applications is crucial. This paper introduces a novel approach using parameterization to find the optimal thickness within a defined range. ANSYS Workbench is utilized for conducting para-metric analyses, enabling the automatic solution of various thickness values to identify critical points, trends, and key design parameters. The forceps' thickness is treated as a variable parameter in the optimization process. The primary objectives are to minimize equivalent stress and maximize output deformations, enhancing overall performance and efficiency. The optimization problem considers constraints such as boundary and loading conditions, ensuring practical feasibility and functionality of the mechanism.

Through systematic manipulation of the thick-ness parameter and examination of the resulting stress and deformation outcomes, the suggested approach facilitates a thorough comprehension of the intricate relationship between thickness variations and mechanical performance. This detailed analysis offers valuable insights into the design domain, assisting in identifying optimal thickness values that achieve a harmonious equilibrium between structural integrity and the intended deformations in the planar mechanism.

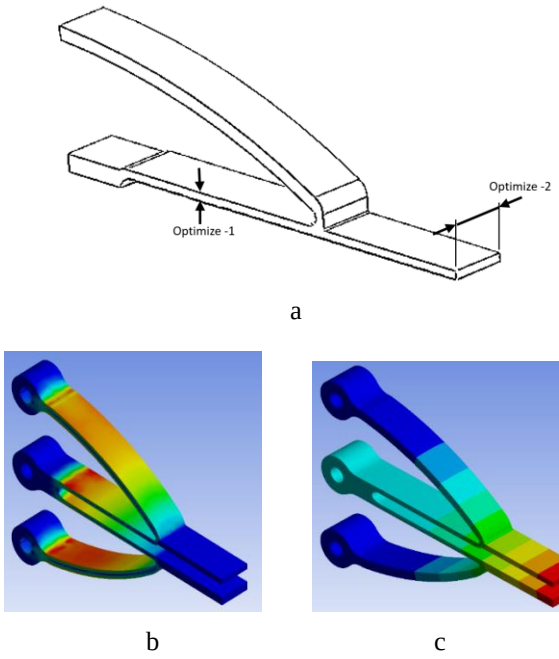

Fig. 4 FE Models: a – parametric model, b – equivalent stress, c – total displacement

The contour plot of the finite element analysis for various optimal parameter is depicted in Fig. 4, a (refer to Table 1). In contrast to a flexure-hinged-based compliant mechanism, the equivalent stress at Fig. 4, b is uniformly distributed. Fig. 4, c reveals that the maximum total deformation occurs at the tip of the forceps, indicating that the kinematic configuration is effective and ensures that the maximum output occurs at the tip.

Table 1

Table of design points

Sl No:	Optimize -1, mm	Optimize -2, mm	Force, N	Equivalent Stress, MPa	Deformation, mm
1	0.6	5	25	229.65	0.59083
2	0.9	5	25	221.49	0.38246
3	0.8	5	25	194.79	0.44218
4	0.7	5	25	202.85	0.51247
5	0.6	5	25	229.65	0.59083
6	0.5	5	25	218.01	0.67139
7	0.6	4.75	25	242.53	0.62263
8	0.6	4.5	25	256.75	0.65795
9	0.6	4.25	25	272.52	0.69744
10	0.6	4	25	290.02	0.74183
11	0.6	3.75	25	309.86	0.79218
12	0.6	3.5	25	332.27	0.84971

In the parameterization process, 12 design points are extracted for the variable thickness, ranging from 3 to 5 mm with a 0.25 mm interval. The thickness range is selected based on commercially available forceps. Table 1 presents the equivalent stress and maximum deformation of the finite element model for these 12 design points. From these values, 0.6 mm for part 1 and 4 mm for part 2 are identified as optimal for the current product. It is noteworthy that

if the thickness is less than 3 mm, stress increases drastically; hence, analysing below this thickness is deemed unnecessary.

Fig. 5 illustrates the final product, featuring three holes designed for attachment to a handle or any standard fixture. The portable attachment incorporates an adjustable mechanism in the propeller to achieve the necessary linear travel. It is designed to be compact enough to be easily held in one hand.

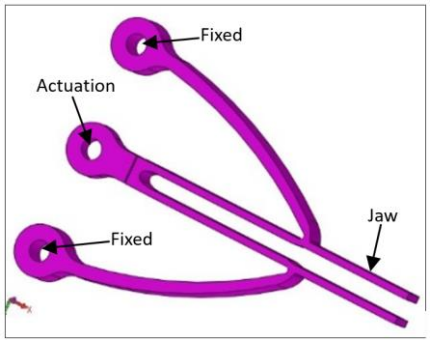

Fig. 5 Final design of forceps

3. Experimental Investigations

The objective of this experiment is to explore the structural capabilities of the recently introduced compliant forceps. Output displacement is assessed through a vision system, while a flexible pressure sensor is employed to gauge the gripping force during contact. The compliant forceps are crafted using the wire EDM technique (Electrical Discharge Machining) with exceptional precision. Fig. 6 illustrates compliant forceps crafted from medical-grade stain-less steel 304, which has undergone post-processing for refinement.

Fig. 7, a and b illustrates the block diagram and experimental setup designed for assessing the output deformation of the microgripper. The setup involves creating a specialized stage to secure both piezo actuators and compliant forceps. This stage is securely affixed to an adjacent stage. A USB cable establishes a connection between the servo controller and the PC, facilitating communication with the piezo actuator.

3.1. Evaluation of deflection for the gripper

For real-time observation of the gripper's motion during operation, a high-resolution camera, integrated with the microscope, is linked to a computer. The collected images are then analysed using the micro measurement

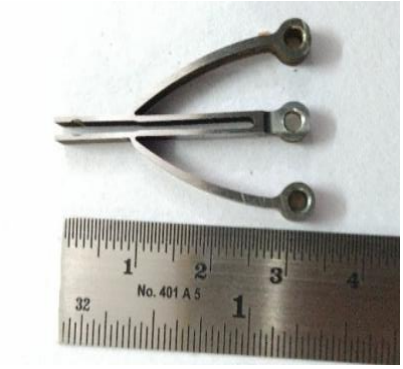

Fig. 6 Compliant forceps prototype

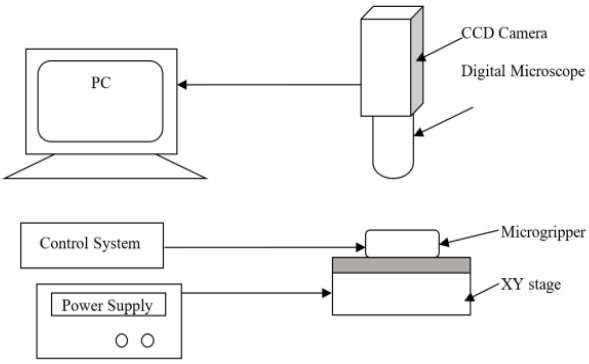

a

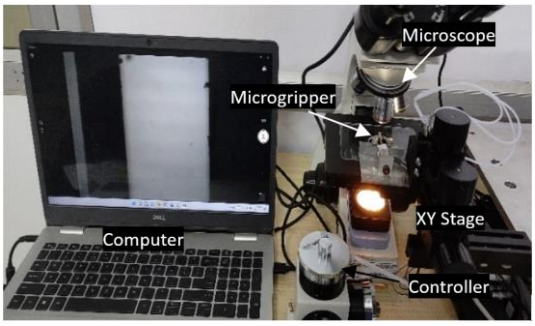

b

Fig. 7 Experimental analysis: a – block diagram, b – experimental setup

software embedded in the microscope. This comprehensive arrangement enables precise monitoring and evaluation of the microgripper's performance.

The piezo actuator exhibits a maximum input displacement capability of 15 mm when subjected to an applied voltage. The resulting displacement of the microgripper is observed through a microscope, as illustrated in Fig. 8. Subsequently, the micro measurement software is employed to measure the captured images of the initial and actuated states. Fig. 9 visually represents the output displacement at the gripper's tip across different input displacements. Notably, the alignment between the outcomes obtained from finite element analysis and experimental analysis is evident, highlighting a concurrence between the theoretical predictions and the practical observations.

3.2. Gripping force measurement of jaws

The development of a compliant mechanism design involves a focus on estimating gripping force during manipulation. An experimental investigation is conducted to ascertain the gripping force, as depicted in Fig. 10. In this scenario, a gripper is utilized to grasp a rigid object, and during the gripping process, the thin jaw undergoes deflection. The images captured before and after gripping are analyzed, and motion is quantified using software, as demonstrated in Fig. 11. Before clamping, the gap between the jaw’s measures 1.67 mm, and after clamping, it increases to 1.69 mm.

Numerical analysis has been employed to anticipate the reaction force acting on an object, closely resembling the gripping force. From image-based measurements,

the observed deflection is recorded at 0.02 mm. Concurrently, employing the beam equation yields a calculated gripping force of 0.3447 N. To validate these findings, a Finite Element Method (FEM) study is conducted. The FEM analysis reveals a reaction force of 0.3547 N, as depicted in Fig. 12. Correspondingly, the maximum deflection in this FEM study is estimated to be 0.024 mm.

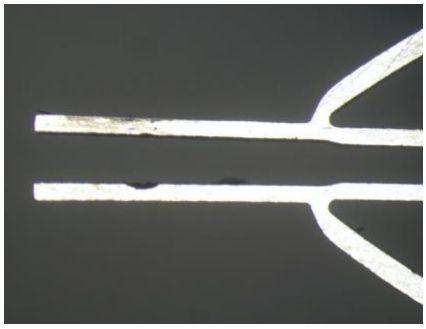

Fig. 8 Output image

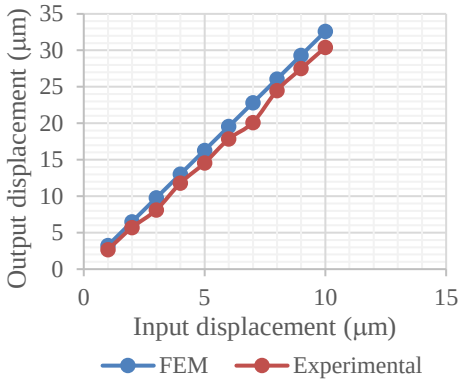

Fig. 9 Output displacement of gripper

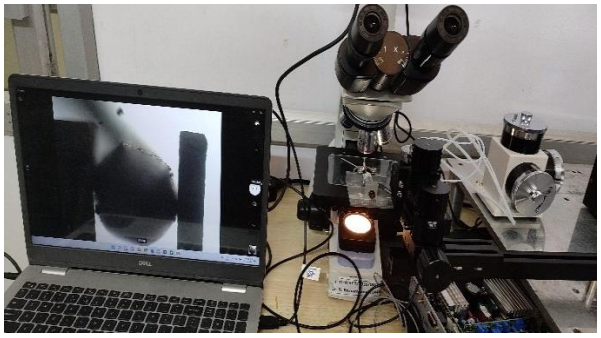

Fig. 10 Experimental set up

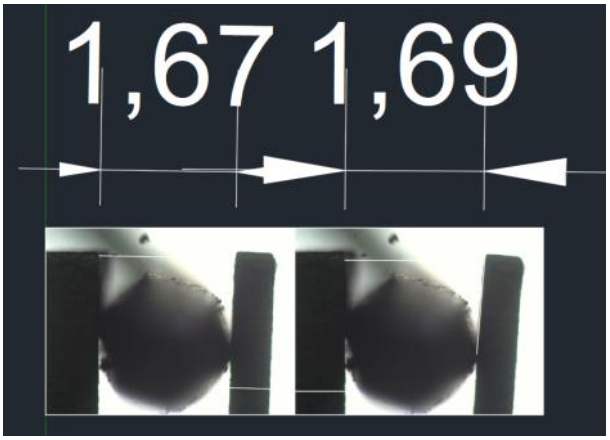

Fig. 11 Jaw gripping action initial and activated position

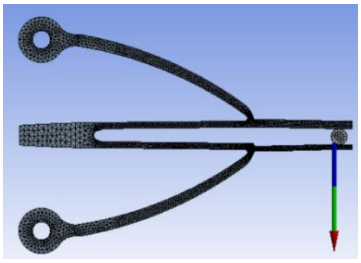

Fig. 12 Force reaction on the rigid object

The deflection analysis for an applied force is conducted using a Microscope-XY stage setup, where the final prototype is affixed to the XY stage using a mechanical clamp. The deflections are quantified through microscopic measurements and organized in Table 2. In particular, when examining Table 2, the numerically obtained deflection for a grip-per with a 0.6 mm thickness for part 1 and a 4 mm width for part 2 is 0.74183 mm, corresponding to an input force of 25 N, or an input deflection of 0.125 mm.

For the assessment, approximately 5 iterations were carried out on the fabricated gripper. Notably, the comparison between numerical predictions and experimental results, as presented in Table 2, reveals a variation of less than 1%. This minute difference is attributed to meticulous considerations such as mesh studies and the careful selection of finite element method (FEM) elements. Attention to detail in these aspects has resulted in a negligible deviation between the numerical and experimental outputs, underscoring the accuracy of the evaluation process.

Table 2
Experimental vs numerical output displacement

Sl No:	Input displacement, mm	Numerical output displacement, mm	Displacement from microscope, mm	Percentage variation
1	0.125	0.74183	0.734967	0.925144575
2	0.125	0.74183	0.735698	0.826604478
3	0.125	0.74183	0.734976	0.923931359
4	0.125	0.74183	0.734956	0.926627394
5	0.125	0.74183	0.734933	0.929727835

3.3. Integration of force sensor

A force measurement system has been designed to quantify gripping force, with its magnitude directly correlated to tissue stiffness. The circuit block diagram, depicted in Fig. 13, comprises essential components, including an Analog-to-Digital Converter (Microcontroller), a Flexible Pressure Sensor, a display board, and a potentiometer. The chosen Analog-to-Digital Converter for the system is the ST Microelectronics NUCLEO-F072RB, a 32-bit microcontroller. This microcontroller is configured with a 12-bit Analog-to-Digital Converter (ADC) capable of accurately measuring voltages as small as 0.8 million volts. The detailed specifications of the NUCLEO-F072RB can be found in Table 3.

The pressure sensor employed in the system is a flexible sensor with a thickness of 0.24 mm and a sensing

Table 3

Specification of analog-to-digital converter

Product Attribute	Attribute Value
Manufacturer of Part:	STMicroelectronics
Category of Product:	Development Boards & Kits - ARM
Series:	NUCLEO - F072RB
Core:	ARM Cortex M0
Interface Type:	USB
Data Bus Width:	32 bits
Operating Supply Voltage:	3.3 V

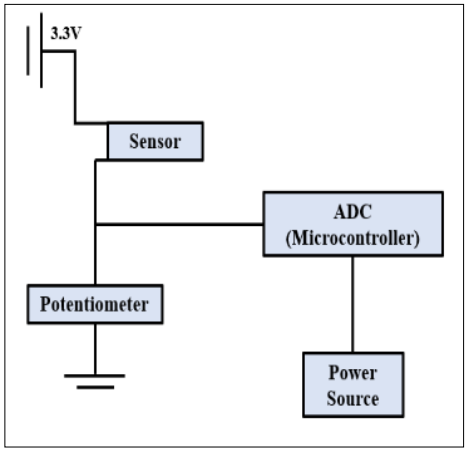

Fig. 13 Circuit block diagram

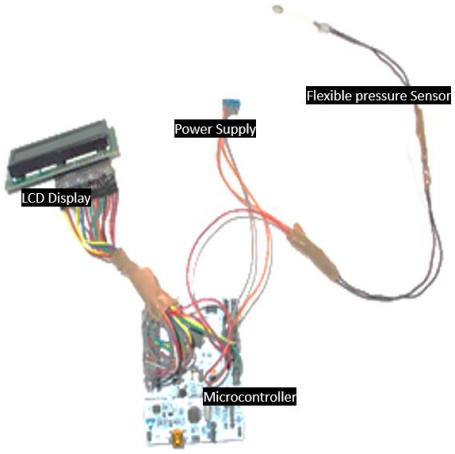

Fig. 14 Measuring system

diameter of 4 mm. The sensor's specifications are outlined in Table 4. To provide a user-friendly interface and display the relevant information, a 16 x 2 LCD Display with Blue Backlight, as depicted in Fig. 14, is utilized in the system. In summary, the force measurement system incorporates a sophisticated setup with a powerful microcontroller, a flexible pressure sensor, and a clear display, enabling accurate and efficient measurement of gripping force in relation to tissue stiffness.

The LCD display records sensor output voltage corresponding to different input displacements of the gripper. Concurrently, Finite Element Analysis (FEA) was conducted to analyze and quantify the re-action force observed at the tip of the gripper's jaw. Fig. 15 illustrates the plotted values of sensor output voltage in Volts against reaction force in Newton. By analyzing the curves, it becomes evident that there is a direct proportionality between the sensor output and the reaction force.

Table 4

Specification of the pressure sensor

Product Attribute	Attribute Value
Actuation Force required	0.1 Newtons
Force Sensitivity	0.1 – 10.02 Newtons
Resistance on non-Actuation	10 M W
Repeatability	±5.8 (50% load)
Lifespan	1 Million cycle
Device Rise Time	Less than 3 microseconds
Operating Temperature (°C)	-30 to 60
Clock-Speed	16 MHz
Flash-Memory	32 KB
Overall length	45 mm
Overall width	7 mm
Sensing area	4 mm

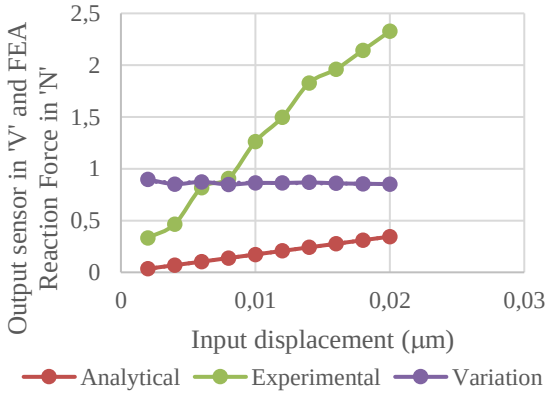

Fig. 15 FEA reaction force and sensor output against input displacement

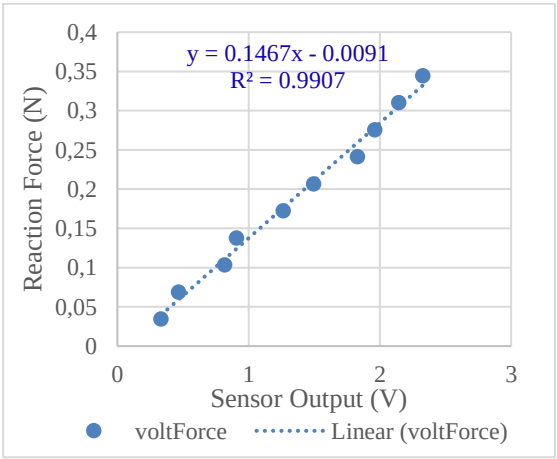

Fig. 16 Calibration plot between sensor outputs against Reaction force

A detailed examination of the variation between the curves has been performed and graphically represented. The calculated variation curve distinctly demonstrates that the reaction force maintains a consistent proportionality to the sensor output. This variation, depicted graphically, falls within the range of 85% to 87%, indicating a stable relationship. The curve, essentially horizontal, underscores the reliability of the experimental results, signifying a consistent and predictable correlation between sensor output and reaction force. The measured reaction force during gripping serves as an indication of the gripping force.

Fig. 16 depicts the relationship between sensor output and the reaction force obtained from Finite Element Analysis (FEA). This curve, shown in Fig. 16, is utilized for calibrating the instruments. The equation for determining gripping force in terms of voltage is expressed as follows:

$$y = 0.1467x - 0.0091 \text{ with } R^2 = 0.9907, \quad (2)$$

where, y represents gripping force in N, x represents sensor output in V.

4. Conclusion

This project focuses on the development of an innovative gripper or forceps with the added capability of measuring gripping force. The key design principle employed is the utilization of a compliant mechanism, chosen for its ability to provide high precision and force feedback during manipulations. The design of the planar kinematic configuration is achieved through topology optimization, resulting in a distributed compliant mechanism. To enhance the precision and functionality of the gripper, parameterization techniques are applied to determine the optimal thickness of the device. This hybrid approach, combining topology optimization and parameterization, represents a novel and effective strategy that has led to significant improvements in the design. The designed gripper is not confined to theoretical concepts but is further developed into a practical handheld device. Manufacturing is carried out using the wire EDM (Electrical Discharge Machining) process, ensuring the feasibility of the proposed design.

A crucial aspect of the project involves the integration of a force sensor module directly into the gripper. This module allows for the measurement of gripping force in terms of proportional voltage. Calibration of the forceps and sensor system is conducted using Finite Element Analysis (FEA) results and an equation with a high coefficient of determination (R2 = 0.9907), validating the accuracy and reliability of the prototype. Beyond its gripping capabilities, the developed device holds promise as a significant tool for medical applications. In addition to conventional testing methods such as CT (computed tomography) or MRI (magnetic resonance imaging) scans, this de-vice serves as a secondary tool, providing additional valuable information about tissues during manipulation. This dual functionality positions the prototype as a versatile and indispensable instrument in various fields, particularly in medical contexts where precision and real-time feedback are critical.

Conflict of interest

The Authors declares that there is no conflict of interest.

Funding

Science and Engineering Research Board (SERB) India supports this work through Early Career Research (ECR) Award scheme (ECR/2016/001938).

References

1. **Liu C.-H., Huang G.-F., Chiu C.-H., Pai T.-Y**. 2018. Topology Synthesis and Optimal Design of an Adaptive Compliant Gripper to Maximize Output Displacement, Journal of Intelligent & Robotic Systems 90: 287-304. https://doi.org/10.1007/s10846-017-0671-x.
2. **Hoover, A. M.; Fearing, R., S.** 2007. Rapidly Prototyped Orthotweezers for Automated Microassembly, Proceedings 2007 IEEE International Conference on Robotics and Automation: 812-819. https://doi.org/10.1109/ROBOT.2007.363086.
3. **Henke, A.; Kümmel, M. A.; Wallaschek, J.** 1999. A piezoelectrically driven wire feeding system for high performance wedge-wedge-bonding machines, Mechatronics, 9(7): 757-767. https://doi.org/10.1016/S0957-4158(99)00025-2.
4. **Howell, L. L.** 2001. Compliant Mechanisms. New York: John Wiley & Sons. 480p.
5. **Saggere, L.; Kota, S.** 2001. Synthesis of Planar, Compliant Four-Bar Mechanisms for Compliant-Segment Motion Generation, ASME Journal of Mechanical Design 123(4): 535–541. https://doi.org/10.1115/1.1416149.
6. **Bendsøe, M. P.; Sigmund O.** 2004. Topology Optimization: Theory, Methods and Applications. Berlin: Springer-Verlag. 370p. https://doi.org/10.1007/978-3-662-05086-6.
7. **Bharanidaran, R.; Ramesh, T**. 2014. Numerical simulation and experimental investigation of a topologically optimized compliant microgripper, Sensors and Actuators A: Physical 205: 156-163. https://doi.org/10.1016/j.sna.2013.11.011.
8. **Albanesi, A. E.; Fachinotti, V. D.; Cardona, A.** 2010. Inverse finite element method for large displacement beams, International Journal for Numerical Methods in Engineering 84(10): 1166-1182. https://doi.org/10.1002/nme.2935.
9. **Reddy, A. N.; Maheshwari, N.; Sahu, D. K.; Ananthasuresh, G. K.** 2010. Miniature Compliant Grippers With Vision-Based Force Sensing, IEEE Transactions on Robotics 26(5): 867–877. https://doi.org/10.1109/TRO.2010.2056210.
10. **Lan, C.-C.; Wang, J.-Y.** 2011. Design of adjustable constant-force forceps for robot-assisted surgical manipulation, in Proc. IEEE International Conference on Robotics and Automation: 386–391. https://doi.org/10.1109/ICRA.2011.5979556.
11. **Hong, M. B.; Jo Y.-H.** 2012. Design and Evaluation of 2-DOF Compliant Forceps With Force-Sensing Capability for Minimally Invasive Robot Surgery, IEEE Transactions on Robotics 28(4): 932-941. https://doi.org/10.1109/TRO.2012.2194889.
12. **Alambeigi, F.; Bakhtiarinejad, M.; Sefati, S.; Hegeman, R.; Iordachita, I; Khanuja, H.; Armand, M**. 2019. On the Use of a Continuum Manipulator and a Bendable Medical Screw for Minimally Invasive Interventions in Orthopedic Surgery, IEEE Transactions on Medical Robotics and Bionics 1(1): 14–21. https://doi.org/10.1109/TMRB.2019.2895780.
13. **Z. Wu, Q. Li, J. Zhao, J. Gao, and K. Xu**. 2019. Design of a modular continuum-articulated laparoscopic robotic tool with decoupled kinematics, IEEE Robot. Autom. Lett., 4, 3545–3552.
14. **Kota, S.; Lu, K.-J.; Kreiner, Z.; Trease, B.; Arenas, J.; Geiger, J.** 2005. Design and application of compliant mechanisms for surgical tools, Journal of Biomechanical Engineering 127(6): 981-989.

https://doi.org/10.1115/1.2056561.
15. **Sun, Y.; Liu, Y.; Xu, L.; Zou, Y.; Faragasso, A.; Lueth, T. C.** 2020. Automatic Design of Compliant Surgical Forceps With Adaptive Grasping Functions, IEEE Robotics and Automation Letters 5(2): 1095-1102. https://doi.org/10.1109/LRA.2020.2967715.
16. **Frecker, M. I.; Dziedzic, R. P.; Haluck, R. S.** 2002. Design of multifunctional compliant mechanisms for minimally invasive surgery, Minimally Invasive Therapy & Allied Technologies 11(5-6): 311–319. https://doi.org/10.1080/13645706.2003.11873732.
17. **George, L. B.; Bharanidaran, R.** 2020. Design of multifunctional compliant forceps for medical application, Australian Journal of Mechanical Engineering 20(3): 731-735. https://doi.org/10.1080/14484846.2020.1747151.
18. **de Lange, D. J.; Langelaar, M.; Herder J. L.** 2008. Towards the Design of a Statically Balanced Compliant Laparoscopic Grasper Using Topology Optimization, Proceedings of the ASME 2008 International Design Engineering Technical Conferences and Computers and Information in Engineering, 32nd Mechanisms and Robotics Conference, Parts A and B 2: 293–305. https://doi.org/10.1115/DETC2008-49794.
19. **Salerno, M.; Zhang, K.; Menciassi, A.; Dai, J. S.** 2016. A Novel 4-DOF Origami Grasper With an SMA-Actuation System for Minimally Invasive Surgery, IEEE Transactions on Robotics 32(3): 484-498. https://doi.org/10.1109/TRO.2016.2539373.
20. **Tholey, G.; Pillarisetti, A.; Green, W.; Desai, J. P.** 2004. Design, Development, and Testing of an Automated Laparoscopic Grasper with 3-D Force Measurement Capability, In: Cotin, S., Metaxas, D. (eds) Medical Simulation, ISMS 2004, Lecture Notes in Computer Science vol 3078: 38-48. https://doi.org/10.1007/978-3-540-25968-8_5.
21. **Rosen, J.; Hannaford, B.; MacFarlane, M. P.; Sinanan, M. N.** 1999. Force controlled and teleoperated endoscopic grasper for minimally invasive surgery-experimental performance evaluation, IEEE Transactions on Biomedical Engineering 46(10): 1212–1221. https://doi.org/10.1109/10.790498.
22. **Xu, W.; Zhang, H.; Yuan, H.; Liang, B.** 2021. A Compliant Adaptive Gripper and Its Intrinsic Force Sensing Method, IEEE Transactions on Robotics 37(5): 1584-1603, https://doi.org/10.1109/TRO.2021.3060971.

G. Vijayan, B. Ramalingam, L. G. Babu,
A. Masilamany Santha

A NEW TWO-PHASE DESIGN PROCESS FOR A COMPLIANT MECHANISM GRIPPER

S u m m a r y

Precision industries focus on achieving high accuracy and controllable motion in the structural design of components. Compliant mechanisms have emerged as a preferred choice among researchers, as they enable motion without relying on traditional joints. These compliant mechanisms, lacking hard junctions, facilitate the construction of microscale devices. This study introduces a novel two-phase de-sign methodology for compliant mechanism forceps, aiming to eliminate high-stress areas by employing a distributed compliant mechanism. The forceps design incorporates topological optimization with a new approach to create a distributed planar design. The introduction of a design domain with a pattern of holes restricts single point contact formation and promotes the formation of a distributed compliant mechanism. A parameterization technique is implemented to transition from conceptual design to a functional working design. The compliant forceps design is rigorously evaluated through finite element analysis (FEA) based on structural considerations. The research culminates in the development of a handle-equipped microgripper prototype. Experimental verification showcases the gripper's performance, revealing a variation of less than 3% compared to numerical results. An integrated force sensor measures gripping force, and the results are compared with the reaction force estimated through FEA. This comprehensive approach to compliant mechanism forceps design and evaluation contributes valuable insights to the field of precision industries.

Keywords: compliant mechanism, forceps, topology optimization, flexure hinges.

Received March 10, 2023
Accepted October 22, 2024